Absence of Proteinase-Activated Receptor-1 Signaling in Mice Confers Protection from fMLP-Induced Goblet Cell Metaplasia

Luigi Atzori[1]*, Monica Lucattelli[2]*, Chris J. Scotton[3], Geoffrey J. Laurent[3], Barbara Bartalesi[2], Giovanna De Cunto[2], Benedetta Lunghi[2], Rachel C. Chambers[3‡], and Giuseppe Lungarella[2‡]

[1]Department of Toxicology, University of Cagliari, Cagliari, Italy; [2]Department of Physiopathology and Experimental Medicine, University of Siena, Siena, Italy; and [3]Centre for Respiratory Research, University College London, London, United Kingdom

The morphological features of chronic obstructive pulmonary disease in man include emphysema and chronic bronchitis associated with mucus hypersecretion. These alterations can be induced in mice by a single intratracheal instillation of N-formyl-L-methionyl-L-leucyl-L-phenylalanine (fMLP), a chemoattractant and degranulating agent for neutrophils. The mechanisms underlying excessive mucus production and, in particular, goblet cell hyperplasia/metaplasia in chronic obstructive pulmonary disease remain poorly understood. The proteinase-activated receptors (PARs) are widely recognized for their modulatory properties during inflammation. In this study, we examined whether PAR-1 contributes to inflammation and lung damage induced by fMLP by comparing the response of PAR-1–deficient (PAR-1$^{-/-}$) mice with that of wild-type (WT) mice. Mice were killed at various time points after fMLP instillation (200 μg/50 μl). WT mice developed emphysema and goblet cell metaplasia. The onset of pulmonary lesions was preceded by an increase in thrombin immunoreactivity in bronchial airways and alveolar tissue. This was followed by a decrease in PAR-1 immunoreactivity, and by an increase in IL-13 immunostaining on the luminal surface of airway epithelial cells. In PAR-1$^{-/-}$ mice, fMLP administration induced similar responses in terms of inflammation and emphysema, but these mice were protected from the development of goblet cell metaplasia. The involvement of PAR-1 in airway epithelial cell transdifferentiation was confirmed by demonstrating that intratracheal instillation of the selective PAR-1 agonist (TFLLR) induced goblet cell metaplasia in the airways of WT mice only. These data suggest that emphysema and goblet cell metaplasia occur independently, and that PAR-1 signaling through IL-13 stimulation may play an important role in inducing goblet cell metaplasia.

Keywords: goblet cell metaplasia; emphysema; proteinase-activated receptor-1; IL-13; epidermal growth factor receptor

Chronic obstructive pulmonary disease (COPD) is a major and increasing global health problem. Morphological features of COPD include emphysema (airspace enlargement due to destruction of the lung parenchyma) and chronic bronchitis associated with mucus hypersecretion. A central pathogenetic role in COPD has been attributed to the inflammatory response that is present throughout the airways and parenchyma, and which participates in the progression and exacerbation of this disease (1). Neutrophils and macrophages release mediators that contribute to inflammation and overwhelm lung defenses (2, 3). These mediators can injure the alveolar walls by activating program(s) for lung destruction (emphysema), and/or can remodel the airways by inducing goblet cell metaplasia (3). Although the mechanisms of hypersecretion are not fully understood, increased mucus secretion is currently attributed to hypertrophy and hyperplasia of bronchial submucosal glands and goblet cell hyperplasia/metaplasia in the airway epithelium (4). In the bronchial epithelium, the reduction of ciliated cells in favor of goblet cells may further contribute to the impaired mucociliary transport responsible for airway obstruction. Unfortunately, the inflammatory pathway(s) and the mediators involved in the pathogenesis of COPD have not yet been clearly defined (5), although both epidermal growth factor receptor (EGFR) activation and IL-13 signaling have been highlighted as potential key pathways involved in the development of goblet cell hyperplasia and metaplasia. In particular, by using a model of Sendai virus infection and analysis of patients with asthma, Tyner and coworkers (6) recently demonstrated that goblet cell metaplasia derives from ciliated cell transdifferentiation, and requires two signals. The first signal activates EGFR, which leads to inhibition of ciliated cell apoptosis and cell survival; the second signal is mediated by IL-13 acting via its receptor to promote ciliated cell transdifferentiation into mucus-producing goblet cells. It also appears that other epithelial cells, such as Clara cells, can differentiate into goblet cells through the same pathway (6).

At present, the contribution of the coagulation cascade to the development of COPD remains unclear, but plasma levels of procoagulant and fibrinolytic markers are elevated in patients with COPD (7). The presence of microthrombi within the vasculature of patients with COPD further suggests that COPD is associated with a procoagulant state.

Thrombin, a trypsin-like serine protease, plays a central role in blood coagulation, and also mediates a number of biological responses that may play important roles in inflammatory and tissue repair responses (8). Most of the cellular effects of

CLINICAL RELEVANCE

The mechanisms underlying excessive mucus production and, in particular, goblet cell hyperplasia/metaplasia in chronic obstructive pulmonary disease remain poorly understood. We show that proteinase-activated receptor (PAR)-1 signaling may play an important role in inducing goblet cell metaplasia in this model. PAR-1 may offer promise as a novel target for interfering with mucus hypersecretion.

(*Received in original form October 26, 2007 and in final form February 16, 2009*)

* These authors contributed equally.

‡ These authors contributed equally.

This work was supported in part by Ministero dell'Istruzione, dell' Università e della Ricerca, Rome, Italy, grant 2004067923 (M.L.); Ministero dell'Istruzione, dell' Università e della Ricerca, Rome, Italy, grant RBIP06YM29_004 (G.L.); and Banco di Sardegna Foundation grant 3072005.0042 (L.A.). C.J.S. was funded by Wellcome Trust Program grant GR071124MA.

Correspondence and requests for reprints should be addressed to Rachel C. Chambers, Ph.D., University College London, Rayne Institute, 5 University Street, London WC1E 6JJ, UK. E-mail: r.chambers@ucl.ac.uk

Am J Respir Cell Mol Biol Vol 41. pp 680–687, 2009
Originally Published in Press as DOI: 10.1165/rcmb.2007-0386OC on March 23, 2009
Internet address: www.atsjournals.org

thrombin are mediated by a unique family of ubiquitously expressed cell surface receptors, termed proteinase-activated receptors (PARs). To date, four PARs have been characterized, of which three (PAR-1, -3, and -4) are activated by thrombin. In addition, PAR-1 can also be activated by other coagulation and noncoagulation proteinases, including coagulation factor Xa (9), matrix metalloproteinase-1 (10), and neutrophil elastase (NE) (11). However, the physiological relevance of these activators *in vivo* remains to be established, and the role of PAR-1 in COPD is currently unknown.

PAR-1 is highly expressed by a number of cell types present in the lung, including smooth muscle cells, fibroblasts, endothelial cells, epithelial cells, and macrophages (12). PAR-1 activation has been shown to be both proinflammatory and profibrotic via the release of a host of secondary mediators. The central role for PAR-1 in the injured lung was recently demonstrated in experiments showing that PAR-1 knockout mice are protected from lung inflammation and lung collagen accumulation in the bleomycin model of pulmonary fibrosis (13).

Cigarette smoke (CS) is the main causative factor of COPD in humans. Chronic exposure to CS in sensitive mice reproduces some important changes (i.e., emphysema and goblet cell metaplasia), which characterize COPD in humans. These alterations can also be induced in mice by a single intratracheal instillation of the neutrophil chemoattractant and degranulating agent, N-formyl-L-methionyl-L-leucyl-L-phenylalanine (fMLP) (14, 15). The focus of the current study was to examine the contribution of PAR-1 to fMLP-induced pulmonary alterations by comparing the response obtained in PAR-$1^{-/-}$ and wild-type (WT) mice.

MATERIALS AND METHODS

Animals

WT and PAR-$1^{-/-}$ mice were bred at University College London. All animal studies were approved by the University College London Biological Services Ethical Review Committee and licensed under the Animals (Scientific Procedures) Act 1986, Home Office, London, United Kingdom. Mice were anesthetized with inhaled halothane (3%) in a stream of oxygen (2 L/min) before intratracheal instillation. Mice were housed in specific pathogen-free conditions, and all procedures were performed on male mice between 8 and 12 weeks of age. The generation and backcrossing of PAR-$1^{-/-}$ mice for 10 generations (>97%) onto the C57BL/6 background has been described previously (16, 17).

fMLP Model

Experiments were performed with three groups of eight animals for each strain (WT and PAR-$1^{-/-}$). The first group received a single intratracheal instillation of 200 μg fMLP in 50 μl saline solution. The second group was instilled intratracheally with the same volume of saline. A third group was left untreated. At different time points (1, 3, 7, 14, and 21 d), mice from all groups were terminally anesthetized by an intraperitoneal injection of 100 μl of pentobarbitone sodium (200 mg/ml; Sanofi Aventis, Guildford, UK).

PAR-1 Agonist Instillation

To assess the direct involvement of PAR-1 signaling in the development of goblet cell metaplasia, four groups of C57BL/6 mice ($n = 10$) were given the selective PAR-1 agonist, TFLLR-amide (TFLLR-NH_2; Bachem, Bubendorf, Switzerland), at three different doses (100 μM, 1 mM, and 5 mM, in 50 μl saline solution), or vehicle alone, by intratracheal instillation. The specificity of this agonist in this model was assessed by examining the effect of TFLLR-NH_2 at 5 mM in PAR-$1^{-/-}$ mice ($n = 5$). Mice were terminally anesthetized at either 7 or 14 days ($n = 5$/group/time point) by an intraperitoneal injection of 100 μl of pentobarbitone sodium (200 mg/ml; Sanofi Aventis). The lungs were excised and processed for histological and immunohistochemical analysis.

Bronchoalveolar Lavage and Cytology

To differentiate and quantify inflammatory cell recruitment to the lungs, five animals of each genotype were killed at 1 day after fMLP instillation. The trachea was isolated and then cannulated with a 20-gauge blunt needle. With the aid of a peristaltic pump (P-1; Pharmacia, Uppsala, Sweden), the lungs were lavaged three times with 0.6 ml normal saline. The average fluid recovery was greater than 95%. Total cell counts were performed using a hemocytometer. Differential counts of 300 cells were performed on slides stained with Diff-Quick (Dade Behring AG, Düdingen, Switzerland).

Lung Histology and Mean Linear Intercept Assessment

The lungs from the different groups of mice were fixed intratracheally with buffered formalin (5%) at a constant pressure of 20 cm H_2O for at least 4 hours. All lungs were then dehydrated, cleared in toluene, and embedded in paraffin wax. Two 7-μm latero-sagittal sections of each lung were cut, dewaxed, and stained with hematoxylin and eosin or periodic acid-Schiff (PAS), according to standard histological protocols. Because there are no goblet cells in the murine bronchi (19), a mouse was considered to have developed goblet cell metaplasia when at least one or more middle-sized bronchi/lung showed positive PAS staining.

Morphometric assessment consisted of the determination of the average interalveolar distance (mean linear intercept [Lm]) (18). For each pair of lungs, 40 histological fields were evaluated both vertically and horizontally. Examination of this number of fields meant that practically the entire lung area of each section was evaluated.

Immunohistochemistry

Lung tissue sections (5 μm) were mounted on glass slides before dewaxing in xylene and rehydrating through an ethanol gradient, according to standard histological procedures, and stained for PAR-1 or thrombin by an immunoperoxidase method. For antigen retrieval, the sections were heated by microwaving for 20 minutes in 0.01 M citrate buffer (pH 6.0) and allowed to slowly cool to room temperature. The sections were pretreated with 3% hydrogen peroxide (Sigma-Aldrich, Milan, Italy) to inhibit endogenous peroxidase activity. All sections were incubated with 3% BSA for 30 minutes at room temperature to block nonspecific antibody binding. They were then incubated overnight at 4°C with the primary antibodies, anti–thrombin receptor (PAR-1) rabbit polyclonal antibody (Santa Cruz Biotechnology, Santa Cruz, CA) diluted 1:50; anti-thrombin goat polyclonal (Santa Cruz Biotechnology) diluted 1:50, anti–IL-13 goat polyclonal antibody (R&D Systems Inc., Minneapolis, MN) diluted 1:20, anti-EGFR rabbit polyclonal antibody (Abcam, Cambridge, UK) diluted 1:100, or anti–phosphorylated EGFR (pEGFR) rabbit polyclonal (Abcam) diluted 1:100. All sections were rinsed and incubated with sheep anti-rabbit IgG or anti-goat IgG for 30 minutes at room temperature. For PAR-1 and thrombin detection, after incubation with the appropriate biotin-conjugated secondary antibody, and, subsequently, with streptavidin/peroxidase solution, color development was performed using 3, 3′-diaminobenzidine tetrahydrochloride (DAB; Vector Laboratories, Burlingame, CA) as a chromogen. For IL-13, EGFR, and pEGFR detection, tissue sections were incubated with the appropriate secondary antibody (Sigma-Aldrich) for 30 minutes at room temperature. The staining was revealed by adding peroxidase–antiperoxidase complex (Sigma-Aldrich) prepared from rabbit or goat serum. Detection was accomplished by incubation in freshly dissolved DAB in 0.03% H_2O_2 in 50 mM Tris/HCl (pH 7.6). For MUC5AC detection, tissue sections were incubated overnight at 4°C with mouse monoclonal antibodies to MUC5Ac (1:25) (Thermo Scientific, Waltham, MA). The M.O.M. immunodetection kit (Vector Laboratories) was used for MUC5AC immunodetection. The Vector M.O.M. immunodetection kit is designed specifically to localize mouse primary monoclonal and polyclonal antibodies on mouse tissues by using a novel blocking agent and reducing undesired background staining. Immunostaining was revealed by using the M.O.M. detection kit with DAB substrate.

Specificity of the signal obtained was confirmed by showing that no positive staining was detectable when the primary antibody was substituted with an equivalent concentration of nonimmune polyclonal IgG, or when it was omitted altogether.

Quantification of Goblet Cell Metaplasia

The total number of cells, as well as the percentage of PAS- or MUC5AC-positive cells, was determined. Lung tissue sections from five C57BL/6 mice belonging to groups treated with fMLP, 1 mM TFLLR-amide, or saline solution at 14 days were (immuno)stained for PAS or MUC5AC. The number of cells in airways that demonstrated PAS or MUC5AC staining was determined by examining eight intrapulmonary airways per section, and counting at least 3,000 cells/section. Data were reported both as the number of positive cells per millimeter of basement membrane, and as the percentage of positive cells per total cells.

Western Blot Analysis

Frozen lungs were pulverized using a pestle and mortar and kept frozen with liquid nitrogen. Equal amounts of powder from different animals were resuspended in 1 ml Triton lysis buffer supplemented with a protease inhibitor cocktail (Complete Mini; Roche Diagnostics, Sussex, UK) in polypropylene tubes. Extracts were incubated for 30 minutes on ice and centrifuged at 12,000 $\times$ *g* for 10 minutes at 4°C, and the supernatants recovered. The protein concentration of the resulting total extracts was determined according to the Bradford method (DC Protein Assay; Bio-Rad Laboratories, Hercules, CA). Equal amounts (50 μg/lane) of protein lysate were separated by 10% SDS-PAGE (after reduction with mercaptoethanol), and transferred onto nitrocellulose membranes. The membranes were blocked in Tris-buffered saline containing 5% BSA and milk for 3 hours at room temperature, then incubated with primary anti-thrombin goat polyclonal (Santa Cruz Biotechnology), diluted 1:100, overnight at 4°C. The membranes were washed with 0.05% Tween 20 in Tris-buffered saline, and incubated with a secondary antibody linked to horseradish peroxidase (1:50,000) (Sigma) for 1 hour. After three additional washes, the membranes were incubated in the Bio-Rad amplification reagent (BAR Western blot Amplification Module; Bio-Rad Laboratories) for 10 minutes, washed, incubated in streptavidin–horseradish peroxidase, and washed again before being incubated in the Opti-4CN substrate (Opti-4CN Substrate Kit; Bio-Rad Laboratories), according to the manufacturer's recommendations, and exposed to X-ray film.

Statistical Analysis

For each parameter, either measured or calculated, the values for individual animals were averaged and the SD was calculated. The significance of the differences between groups was calculated using one-way ANOVA (F-test). A *P* value of less than 0.05 was considered significant.

RESULTS

The early response to fMLP in C57BL/6 mice is characterized by marked neutrophil influx into the alveolar space (Figure 1A), which is followed by the development of widespread emphysema by 21 days (Figure 1B). At 24 hours after fMLP administration, there is an approximately 100-fold increase in bronchoalveolar lavage fluid neutrophils (saline control, $0.11 \pm 0.03 \times 10^5$ versus fMLP treated, $10.61 \pm 1.2 \times 10^5$ cells/ml). Twenty-one days after fMLP instillation, lungs from WT C57BL/6 mice showed diffuse areas of air space enlargement, with destruction of alveolar septae and a resultant increase in the Lm of 47.1 (±2.0) μm from baseline values of 35.9 (±0.5) μm (saline control) ($P < 0.05$). These features were previously observed in C57BL/6 mice under similar experimental conditions (14, 15).

The changes in neutrophil number in BALF (saline control, $0.12 \pm 0.04 \times 10^5$ versus fMLP treated, $11.44 \pm 1.3 \times 10^5$ cells/ml), and lung morphology of PAR-1$^{-/-}$ mice, at 24 hours (Figure 1D) and at 21 days (Figure 1E) after fMLP instillation were similar to those observed for C57BL/6 WT mice. The Lm values for saline and fMLP-treated PAR-1$^{-/-}$ mice were 34.1 (±0.6) μm and 48.5 (±2.1) μm, respectively ($P < 0.05$).

There were no differences in gross lung histological appearance by hematoxylin and eosin between saline-instilled WT and PAR-1$^{-/-}$ mice (Figures 1C and 1F). Of interest, fMLP treatment of C57BL/6 mice induces the development of goblet cell metaplasia, within the epithelium of large (Figure 2A) and middle-sized bronchi (Figure 2B), which can be readily appreciated after PAS staining of sections. Some areas of goblet cell metaplasia can be observed as early as 3 days after fMLP instillation (Figure 2C). To the best of our knowledge, this is the first report of goblet cell metaplasia after fMLP instillation into the mouse lung.

Although fMLP treatment of PAR-1$^{-/-}$ mice induced emphysema to a similar extent to that observed in WT mice, striking differences were found in terms of the development of goblet cell metaplasia. The goblet cell metaplasia that characterizes the bronchial and bronchiolar epithelial changes in WT mice was not observed in PAR-1$^{-/-}$ mice after fMLP challenge (Figures 2D and 2E). For comparison, epithelium from middle- and large-sized bronchi of an untreated PAR-1$^{-/-}$ mouse are reported in Figures 2F and 2G, respectively. No differences in

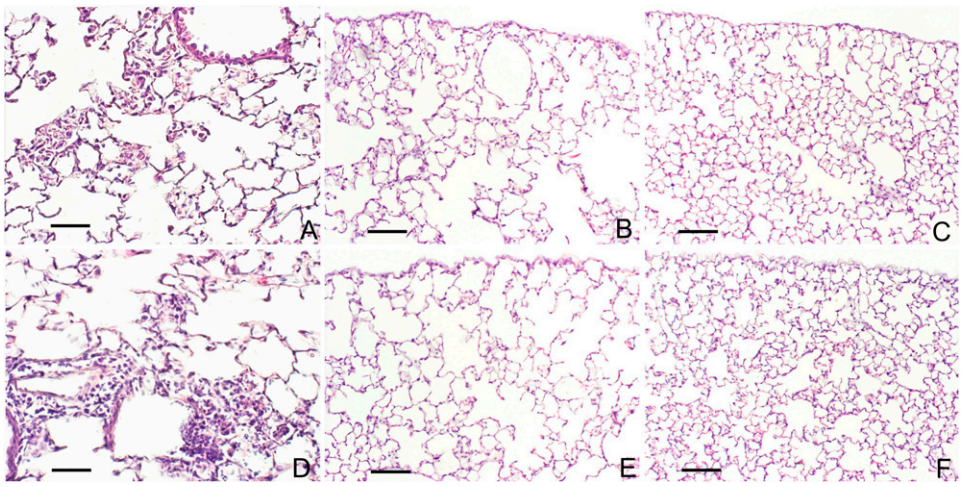

Figure 1. N-formyl-L-methionyl-L-leucyl-L-phenylalanine (fMLP) instillation induces neutrophil infiltration and airspace enlargement in wild-type (WT) and PAR-1–deficient (PAR-1$^{-/-}$) mice. Histological sections from lungs of C57BL/6 and PAR-1$^{-/-}$ mice at 24 hours and 21 days after fMLP instillation are compared with their respective saline-instilled control mice. Representative hematoxylin and eosin (H&E) lung sections of C57BL/6 (*A*) and PAR-1$^{-/-}$ mice (*D*) show consistent neutrophil infiltration into alveolar spaces 24 hours after fMLP instillation. Representative sections of lungs from C57 BL/6 (*B*) and PAR-1$^{-/-}$ (*E*) mice 21 days after fMLP instillation are characterized by diffuse areas of air space enlargement with destruction of alveolar septa. No differences in lung histological appearance are found between saline-instilled WT and PAR-1$^{-/-}$ mice (*C* and *F*). H&E stain; *scale bar*, 170 μm.

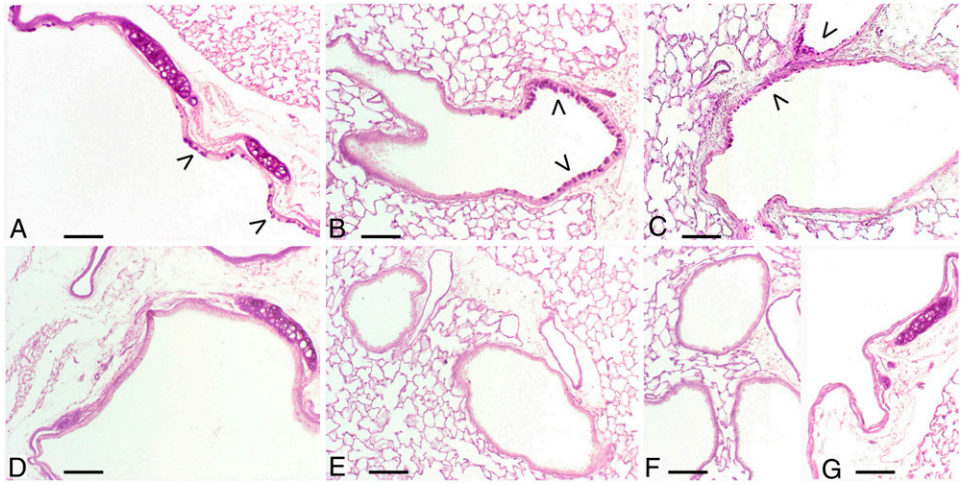

Figure 2. PAR-1$^{-/-}$ mice are protected from fMLP-induced goblet cell metaplasia. Goblet cell metaplasia (*arrowheads*) is appreciable in epithelium of large- (*A*) and middle-sized bronchi (*B*) of WT C57BL/6 mice 21 days after fMLP instillation. Areas of goblet cell metaplasia are found in some C57BL/6 mice as early as 3 days after fMLP treatment (*C*). Bronchial sections of airway epithelium from PAR-1$^{-/-}$ mice at 21 days after fMLP instillation are reported in *D* and *E*. As in saline control mice (*F* and *G*), no periodic acid-Schiff (PAS)–positive cells are present in these sections. PAS stain; *scale bar*, 150 μm.

morphological appearance of airway epithelia were found between control PAR-1$^{-/-}$ and WT mice.

As mentioned above, PAR-1 is highly expressed by a number of cell types present in the lung, including smooth muscle cells, fibroblasts, endothelial cells, epithelial cells, and macrophages (12, 20). Immunohistochemical staining for PAR-1 revealed that this receptor is expressed throughout the lung and airways of C57BL/6 saline-instilled mice (Figures 3A–3C), as previously described (13). In contrast, 1 day after fMLP instillation, immunoreactivity associated with alveolar structures and the bronchial epithelium was markedly reduced (Figures 3D–3F). A return to baseline levels of PAR-1 immunoreactivity can be appreciated within 7 days of fMLP instillation (Figures 3G and 3H).

At Day 1, a time point at which we find the highest reduction in PAR-1 immunoreactivity, we were able to detect thrombin immunoreactivity in pulmonary structures and lung homogenates in fMLP-instilled mice, which was predominately associated with alveolar exudates (Figure 4C) and the surface of bronchial and bronchiolar epithelium (Figure 4D). For comparison, immunostaining of thrombin on alveolar structures (Figure 4A) and bronchial epithelium (Figure 4B) from an untreated WT mouse is reported. The presence of active thrombin is also appreciable by Western blot analysis of lung homogenates from C57BL/6 mice at 1 and 3 days after fMLP instillation (Figure 4E). Taken together these data suggest a possible role for thrombin in the activation of PAR-1 under these experimental conditions.

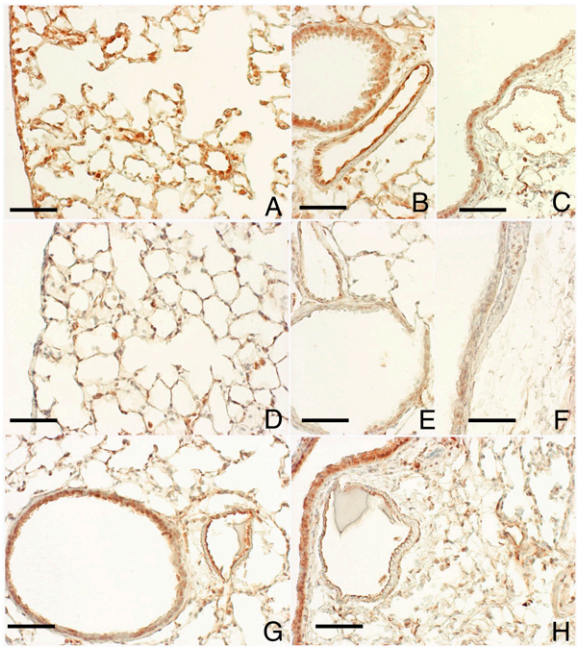

Figure 3. PAR-1 immunoreactivity decreases after fMLP instillation. Immunohistochemical localization of PAR-1 is shown on alveolar and bronchiolar epithelial cells (*A*), on the epithelium of middle- (*B*) and large-size (*C*) bronchi, and on endothelial cells within blood vessels (*B* and *C*) from a control C57BL/6 mouse. In these sections, PAR-1 is consistently expressed throughout the lung parenchyma and airways. In contrast, PAR-1 immunoreactivity associated with the parenchyma (*D*) and airway epithelium (*E* and *F*) is dramatically decreased on Day 1 after fMLP instillation. An almost complete recovery in PAR-1 immunoreactivity is observed throughout the pulmonary structures at 7 days after fMLP instillation (*G* and *H*). *Scale bar*, 100 μm.

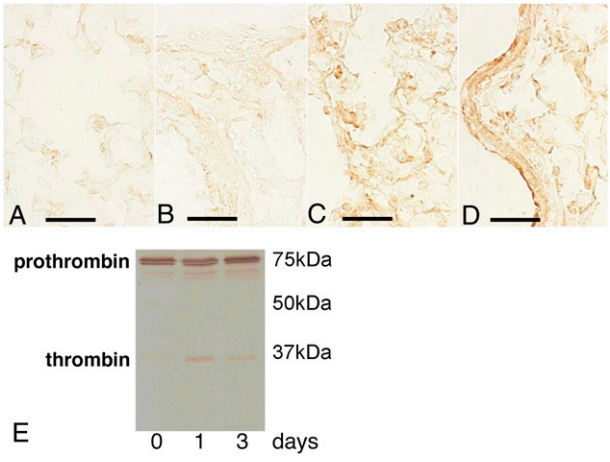

Figure 4. Thrombin immunoreactivity is increased after fMLP exposure. Immunohistochemical localization of thrombin in lung sections from control (*A* and *B*) and fMLP-instilled (*C* and *D*) C57BL/6 mice. Only minimal immunoreactivity is observed within the capillary vessels (*A*) and around the bronchial structures (*B*). At 1 day after instillation of fMLP, there is increased staining for thrombin in alveolar exudates (*C*) and on bronchial epithelial cell surfaces (*D*). *Scale bar*, 75 μm. (*E*) Representative Western blot analysis of thrombin in lung homogenates from C57BL/6 mice at 0, 1, and 3 days after fMLP instillation. Active thrombin is appreciable in lung homogenates at 1 and 3 days after fMLP instillation.

Intratracheal instillation of WT mice with the selective PAR-1 agonist, TFLLR, at three different concentrations (100 μM, 1 mM, and 5 mM) was found to induce goblet cell metaplasia of airway epithelial cells present in middle-sized (Figure 5B) and large bronchi (Figure 5D) at both time points and all concentrations of the agonist examined. In contrast, TFLLR did not induce emphysema/airspace enlargement, even at the highest concentration. The specificity of this agonist in this model was confirmed by demonstrating that TFLLR-NH_2 (5 mM) had no effect in PAR-$1^{-/-}$ mice (n = 5; data not shown). These data suggest that direct PAR-1 signaling in the airways is sufficient to lead to the development of goblet cell metaplasia, but not airspace enlargement.

Goblet cell metaplasia in response to fMLP and TFLLR instillation was also assessed by MUC5AC immunostaining. There was good agreement between the data obtained with PAS and MUC5AC staining in that MUC5AC immunoreactivity was similarly confined to cells present along the airway walls in TFLLR- and fMLP-instilled mice at 7 and 14 days (Figures 5E and 5F). MUC5AC and PAS staining was absent in the lungs of saline-treated control animals. Quantitation of PAS- or MUC5AC-positive cells revealed that around 10% of all airway cells in TFLLR- and fMLP-instilled mice were positive for these goblet cell markers at 14 days after treatment, and, further, that the extent of goblet cell metaplasia was similar for fMLP and TFLLR-instilled mice (Figure 5G). The numbers of PAS- or MUC5AC-positive cells per millimeter basement membrane in the two treatment groups are similarly comparable: 25.5 (±7.1) (PAS) and 21.8 (±6.1) (MUC5AC) for fMLP-instilled mice versus 24.6 (±5.7) (PAS) and 21.1 (±4.9) (MUC5AC) for TFLLR-instilled mice.

Immunohistochemical analysis of IL-13 in mice after intratracheal fMLP revealed that IL-13 was present in the airway epithelium from 1 day onward (Figure 6B), and was predominantly associated with the luminal surface of ciliated cells in middle-sized and large bronchi in WT mice. The airway epithelium demonstrated some positive cytoplasmic staining, as did occasional macrophages, suggesting that these cells may represent a potential cellular source of IL-13 in this model. A similar positive reaction was also observed for WT mice at 7 and 14 days after TFLLR instillation. IL-13 was not detected in saline control groups (Figures 6A and 6C) or fMLP-treated PAR-$1^{-/-}$ mice (Figure 6D).

Immunohistochemical evaluation for EGFR of lung sections from saline control and fMLP-treated groups (WT and PAR-$1^{-/-}$) taken at the various time points revealed no changes in EGFR expression (Figures 7A, 7B, 7D, and 7E) or activation (Figure 7C), as detected by immunostaining for pEGFR between groups. However, pEGFR staining was occasionally found in a very small number of cells in mice challenged with fMLP at 7 days (Figure 7F). Taken together, these data suggest that there is no overlap between EGFR and IL-13 signaling events after fMLP instillation. Similarly, no changes in

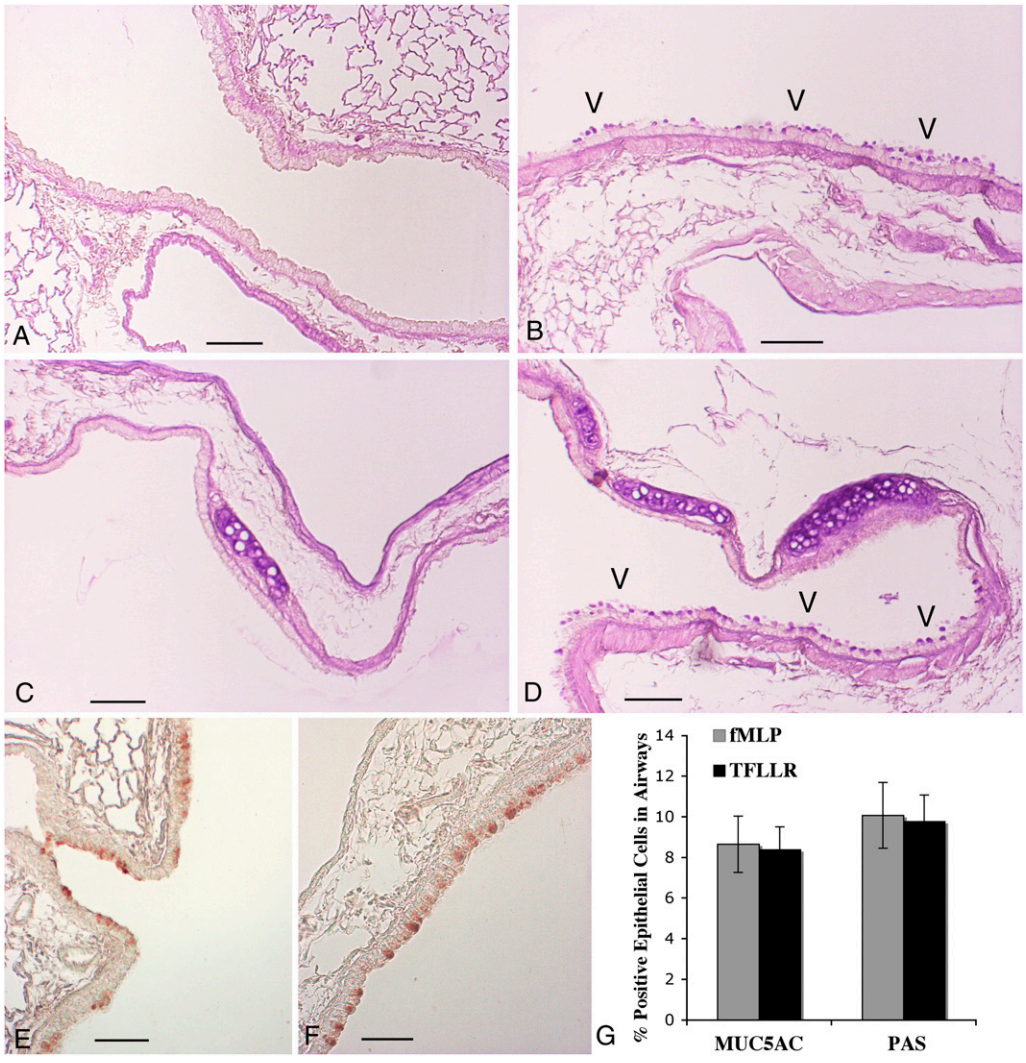

Figure 5. PAR-1 activation induces goblet cell metaplasia in WT mice. PAS staining (*A–D*) of sections demonstrates that goblet cell metaplasia (*arrowheads*) is appreciable within the epithelium of middle- (*B*) and large-sized (*D*) bronchi of WT C57BL/6 mice 14 days after fMLP instillation. Middle-sized and large bronchial sections of airway epithelium from a saline control WT mouse at 14 days after treatment are reported in *A* and *C*. No PAS-positive cells are present in these sections. MUC5AC immunostaining (*E* and *F*) of sections confirms goblet cell metaplasia in fMLP- (*E*) and TFLLR-instilled (*F*) mice. *Scale bar,* 150 μm. (*G*) Quantitation of MUC5AC- and PAS-positive cells in airways from fMLP- and TFLLR-instilled mice at 14 days after treatment. Data are expressed as a percentage of PAS- or MUC5AC-positive airway epithelial cells. Each *bar* represents the mean ± SD (n = 8 intrapulmonary airway sections).

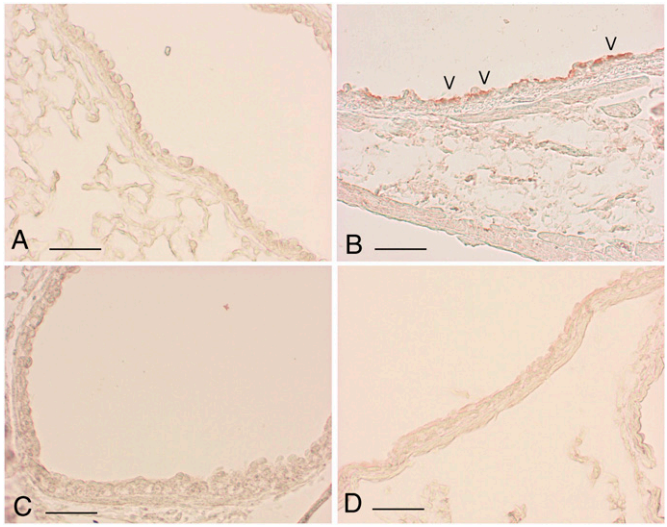

Figure 6. IL-13 immunoreactivity increases after fMLP exposure. IL-13 immunoreactivity was consistently associated with the airway epithelium of WT mice after fMLP treatment from Day 1 onwards. IL-13 immunoreactivity is associated with the luminal surface of epithelial cells within the bronchi (*B*) of WT mice on Day 1 after fMLP instillation (*arrowheads*). IL-13 immunoreactivity is absent in airway epithelium of PAR-$1^{-/-}$ mice at Day 1 after fMLP instillation (*D*). (*A* and C) The airway epithelium for saline control WT and PAR-$1^{-/-}$ mice. IL-13 was undetectable in these sections. *Scale bar*, 150 μm.

EGFR expression or activation were detected after TFLLR instillation (data not shown).

DISCUSSION

Airway remodeling with goblet cell metaplasia, submucosal gland hyperplasia, and mucus hypersecretion are common features of several inflammatory airways diseases, including chronic bronchitis, cystic fibrosis, and asthma (21–23). Mucus hypersecretion as a result of goblet cell hyperplasia causes airway mucus plugging, especially in the peripheral airways, where numerous large secreting goblet cells can more easily cause obstruction (24). The mechanisms underlying excessive mucus production and, in particular, goblet cell hyperplasia/metaplasia in COPD remain poorly understood and highly debated. However, because mucus cell metaplasia in airway diseases is associated with significant airway inflammation, it is generally held that inflammatory cells and their secreted mediators play a central role. A number of stimuli and putative mediators in the induction of goblet cell metaplasia have been considered. These include CS exposure (25), NE (26), IL-1 (27), IL-4 (28), IL-6/IL-17 (29), IL-9 (30), TNF-α (31), LPS (32), uridine 5′-triphosphate (33), as well as IL-13 and EGFR signaling (6).

The main findings of the present study are both the differences and similarities between the C57BL/6 WT and PAR-$1^{-/-}$ mice in response to fMLP instillation. Mice of both experimental groups develop patchy emphysema after fMLP challenge. However, unlike WT mice, PAR-$1^{-/-}$ mice are completely resistant to developing goblet cell metaplasia. These data suggest that emphysema and secretory cell metaplasia in airway epithelium occur independently, and that PAR-1 signaling may play an important role in inducing goblet cell metaplasia in this model. We believe it is unlikely that the lack of goblet cell metaplasia in PAR-$1^{-/-}$ is due to a difference in the extent of the inflammatory response that follows fMLP instillation, because inflammation, characterized by marked neutrophil infiltration and the development of emphysema, are similar in WT and PAR$1^{-/-}$ mice. The involvement of PAR-1 signaling in the development of goblet cell metaplasia was confirmed in additional experiments performed with the specific PAR-1 agonist, TFLLR-NH_2. Intratracheal instillation of this agonist in WT mice lead to goblet cell metaplasia but did not induce the development of emphysematous lesions.

The development of goblet cell metaplasia in WT mice challenged with fMLP or TFLLR-NH_2 was preceded by an increase in IL-13 immunoreactivity without evidence of altered EGFR expression or activation. The presence of IL-13 on the luminal surface of airway epithelial cells, mainly on ciliated cells, is consistent with the proposal that IL-13 may be responsible for promoting the transdifferentiation of ciliated cells to goblet cells downstream of PAR-1 activation in this model. These data are further consistent with a recent report of virus-induced goblet cell metaplasia, where IL-13 on its own was found to be the major mediator responsible for promoting the transdifferentiation of ciliated cells to goblet cells (6). Moreover, this suggestion would also be in agreement with studies of airway epithelial cells, where IL-13 was capable of stimulating goblet cell metaplasia despite EGFR blockade (34). In terms of the cellular source of IL-13 in our model, careful evaluation of

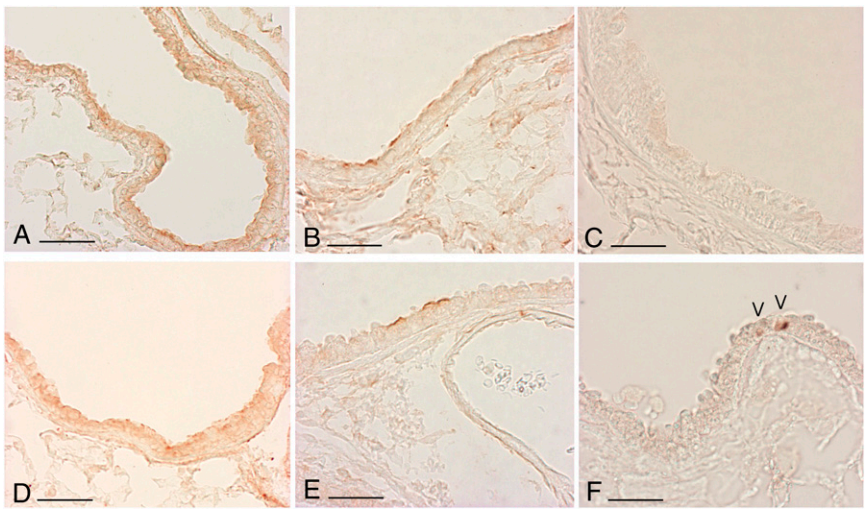

Figure 7. Epidermal growth factor receptor (EGFR) and phosphorylated EGFR (pEGFR) immunoreactivity is unchanged by fMLP exposure. (*A*, *B*, *D*, and *E*) Representative sections immunostained for EGFR from an untreated WT mouse (*A*), a WT mouse at Day 1 after fMLP instillation (*B*), an untreated PAR-$1^{-/-}$ mouse (*D*), and a PAR-$1^{-/-}$ mouse at Day 1 after fMLP instillation. EGFR staining was similar for all groups of mice at all time points examined. *Scale bar*, 150 μm. (*C*) A representative section immunostained for activated EGFR (pEGFR) for WT mice on Day 7 after fMLP treatment. pEGFR immunostaining was similar for all groups of mice at all time points examined. However, positive pEGFR nuclear staining was occasionally found in a very small number of cells in mice belonging to the various experimental groups on Day 7 after fMLP challenge. (*F*) pEGFR nuclear staining (*arrowheads*) in a representative section for PAR-$1^{-/-}$ mice on Day 7 after fMLP treatment. *Scale bar*, 150 μm.

IL-13 immunohistochemistry sections revealed that the airway epithelium and occasional macrophages demonstrated cytoplasmic staining after fMLP challenge. Although this does not allow us to definitively conclude that these cell types represent a cellular source for IL-13 in this model, these cells have been reported to be capable of producing IL-13 *in vitro* (35). Of interest, we also have recent data that IL-13 mRNA levels In PAR1$^{-/-}$ mice are also attenuated in the bleomycin model of lung injury and fibrosis, suggesting that PAR-1 signaling also plays a role in regulating the induction of this cytokine in other lung injury models (A. Naldini, R. J. Johns, and R. C. C., unpublished data). To the best of our knowledge, these are the first *in vivo* reports that there may be cross-talk between PAR-1 and IL-13 signaling pathways. The nature of this cross-talk merits further consideration, and may be relevant in a number of settings characterized by excessive coagulation signaling, abnormal repair, and goblet cell metaplasia.

The potential contribution of PAR-1 to pathological processes in a number of disease settings is increasingly recognized, and several coagulation and noncoagulation proteinases have been implicated in the activation of this receptor, including thrombin, factor Xa, trypsin, plasmin, and matrix metalloproteinase-1 (8). Thrombin inhibition (36) and PAR-1$^{-/-}$ rodent studies (13) suggest that PAR-1 is the main receptor by which thrombin exerts its pluripotent proinflammatory and profibrotic effects after lung injury in the context of fibrotic lung disease. To the best of our knowledge, this is the first report demonstrating the involvement of PAR-1 in the induction of goblet cell metaplasia.

After irreversible proteolytic activation, PAR-1 is rapidly internalized, sorted to lysosomes, and degraded. Internalization and lysosomal sorting of activated PAR-1 is critical for termination of receptor signaling. After agonist exposure, the expression of PAR-1 is markedly reduced for several hours (37) until cell responsiveness is re-established by the mobilization of preformed receptors from intracellular pools, and eventually, the *de novo* synthesis of PAR-1 receptors (38, 39). The transient decrease in PAR-1 immunoreactivity observed at 1 day after fMLP instillation is consistent with the activation and subsequent internalization of this receptor. This may then lead to the induction and release of numerous PAR-1–inducible mediators, including, possibly, IL-13.

After fMLP instillation, the lung response of C57BL/6 mice is characterized by neutrophil influx with the release of NE (14, 15). This mouse strain also develops patchy emphysema and goblet cell metaplasia after chronic exposure to CS (40, 41). These changes are preceded by an increase in PAR-1 mRNA levels, so that PAR-1 may also contribute to emphysema and goblet cell metaplasia after chronic CS exposure (G.L., unpublished data).

In terms of the proteinase responsible for PAR-1 activation in this model, we propose that it is likely that prothrombin leaking into the alveolar space from the vascular compartment, and which is then locally activated to thrombin, is the most likely proteinase involved. Thrombin is generally considered a major physiological and primary activator of PAR-1, with a low EC_{50} of 50 pM, whereas other PAR-1 activators (FXa, trypsin, granzyme A, etc.) are generally considered "secondary activating proteinases," which activate PAR-1 at high concentrations (reviewed in Refs. 8 and 12). It is, however, worth pointing out that NE has also been shown to cleave PAR-1 at both activating (11) and nonactivating sites (42). Furthermore, inflammatory cells and their secreted mediators have been shown to play a central role in several respiratory diseases (e.g., asthma, COPD, cystic fibrosis) (5, 43). These diseases are all characterized by goblet cell metaplasia, and NE is currently considered a major inducer of secretory cell metaplasia via EGFR activation (44) in these conditions. However, whether this proteinase is able to activate PARs *in vivo* remains to be established (37, 45–47). Moreover, immunohistochemical studies to determine the localization of thrombin in our model revealed that, after fMLP administration, there is a consistent positive reaction for thrombin associated with the lung parenchyma and the bronchial epithelium. A quite different localization for NE was observed by us in a previous study performed under identical experimental conditions (14, 15), where elastase could not be detected on the bronchial epithelial cell surface. We therefore propose that thrombin is likely to be the main activator of PAR-1 in this model.

In conclusion, our data show, for the first time, that fMLP instillation induces goblet cell metaplasia, and that PAR-1 signaling plays a key role in experimentally induced goblet cell metaplasia. This appears to be mediated via the local expression of IL-13 without altered EGFR activation. We propose that strategies aimed at blocking PAR-1 may open new avenues for the treatment of mucus hypersecretion in a variety of respiratory conditions.

Conflict of Interest Statement: None of the authors has a financial relationship with a commercial entity that has an interest in the subject of this manuscript.

Acknowledgments: The authors are grateful to Steve Bottoms (Centre for Respiratory Research, University College London) for technical assistance.

References

1. Saetta M, Turato G, Lupi F, Fabbri LM. Inflammation in the pathogenesis of chronic obstructive pulmonary disease. In: Voelkel NF and MacNee W, editors. Chronic obstructive lung disease. Hamilton, ON, Canada: BC Decker; 2002. pp. 114–126.
2. Minematsu N, Shapiro SD. To live and die in the la (lung airway): mode of neutrophil death and progression of chronic obstructive pulmonary disease. *Am J Respir Cell Mol Biol* 2007;37:129–130.
3. Tetley TD. Inflammatory cells and chronic obstructive pulmonary disease. *Curr Drug Targets Inflamm Allergy* 2005;4:607–618.
4. Nadel JA. Mucus and mucus-secreting cells. In: Voelkel NF and MacNee W, editors. Chronic obstructive lung disease. Hamilton, ON, Canada: BC Decker; 2002. pp.161–174.
5. Barnes PJ. Mediators of chronic obstructive pulmonary disease. *Pharmacol Rev* 2004;56:515–548.
6. Tyner JW, Kim EY, Ide K, Pelletier MR, Roswitt WT, Morton JD, Battaile JT, Patel AC, Patterson GA, Castro M, *et al.* Blocking airway mucous cell metaplasia by inhibiting EGFR antiapoptosis and IL-13 transdifferentiation signals. *J Clin Invest* 2006;116:309–321.
7. Ashitani J, Mukae H, Arimura Y, Matsukura S. Elevated plasma procoagulant and fibrinolytic markers in patients with chronic obstructive pulmonary disease. *Intern Med* 2002;41:181–185.
8. Chambers RC. Proteinase-activated receptors and the pathophysiology of pulmonary fibrosis. *Drug Dev Res* 2003;60:29–35.
9. Blanc-Brude OP, Chambers RC, Leoni P, Dik WA, Laurent GJ. Factor Xa is a fibroblast mitogen via binding to effector-cell protease receptor-1 and autocrine release of PDGF. *Am J Physiol Cell Physiol* 2001;281:C681–C689.
10. Boire A, Covic L, Agarwal A, Jaques S, Sherifi S, Kuliopulos A. PAR1 is a matrix metalloprotease-1 receptor that promotes invasion and tumorigenesis of breast cancer cells. *Cell* 2005;120:303–313.
11. Suzuki T, Moraes TJ, Vachon E, Ginzberg HH, Huang TT, Matthay MA, Hollenberg MD, Marshall J, McCulloch CAG, Herrera-Abreu MT, *et al.* Proteinase-activated receptor-1 mediates elastase-induced apoptosis of human lung epithelial cells. *Am J Respir Cell Mol Biol* 2005;33:231–247.
12. Chambers RC. Procoagulant signalling mechanisms in lung inflammation and fibrosis: novel opportunities for pharmacological intervention? *Br J Pharmacol* 2008;153:S367–S378.
13. Howell DCJ, Johns RH, Lasky JA, Shan B, Scotton CJ, Laurent GJ, Chambers RC. Absence of proteinase-activated receptor-1 signaling affords protection from bleomycin-induced lung inflammation and fibrosis. *Am J Pathol* 2005;166:1353–1365.
14. Cavarra E, Martorana PA, Gambelli F, de Santi M, van Even P, Lungarella G. Neutrophil recruitment into the lungs is associated with increased lung elastase burden, decreased lung elastin, and emphysema in alpha 1 proteinase inhibitor–deficient mice. *Lab Invest* 1996;75:273–280.

15. Cavarra E, Martorana PA, de Santi M, Bartalesi B, Cortese S, Gambelli F, Lungarella G. Neutrophil influx in the lungs of beige mice is followed by elastolytic damage and emphysema. *Am J Respir Cell Mol Biol* 1999;20:264–269.
16. Connolly AJ, Suh DY, Hunt TK, Coughlin SR. Mice lacking the thrombin receptor, PAR1, have normal skin wound healing. *Am J Pathol* 1997;151:1199–1204.
17. Cunningham MA, Rondeau E, Chen X, Coughlin SR, Holdsworth SR, Tipping PG. Protease-activated receptor 1 mediates thrombin-dependent, cell-mediated renal inflammation. *J Exp Med* 2000;191: 455–462.
18. Thurlbeck WM. Internal surface area and other measurements in emphysema. *Thorax* 1967;22:483–496.
19. Pack RJ, Al-Ugaily LH, Morris G. The cells of the tracheobronchial epithelium of the mouse: a quantitative light and electron microscope study. *J Anat* 1981;132:71–78.
20. Ossovskaya VS, Bunnett NW. Protease-activated receptors: contribution to physiology and disease. *Physiol Rev* 2003;84:579–621.
21. Rogers DF, Barnes PJ. Treatment of airway mucus hypersecretion. *Ann Med* 2006;38:116–125.
22. Hauber HP, Foley SC, Hamid Q. Mucin overproduction in chronic inflammatory lung disease. *Can Respir J* 2006;13:327–335.
23. Williams OW, Sharafkhaneh A, Kim V, Dichey BF, Evans CM. Airway mucus: from production to secretion. *Am J Respir Cell Mol Biol* 2006; 34:527–536.
24. Dunnill MS. The pathology of asthma, with special reference to changes in the bronchial mucosa. *J Clin Pathol* 1960;13:27–33.
25. Martorana PA, Beume R, Lucattelli M, Wollin L, Lungarella G. Roflumilast fully prevents emphysema in mice chronically exposed to cigarette smoke. *Am J Respir Crit Care Med* 2005;172:848–853.
26. Fisher BM, Voynow JA. Neutrophil elastase induces MUC5AC gene expression in airway epithelium via a pathway involving reactive oxygen species. *Am J Respir Cell Mol Biol* 2002;26:447–452.
27. Lappalainen U, Whitsett JA, Wert SE, Tichelaar JW, Bry K. Interleukin-1β causes pulmonary inflammation, emphysema, and airway remodeling in the adult murine lung. *Am J Respir Cell Mol Biol* 2005;32:311–318.
28. Dabbagh K, Takeyama K, Lee HM, Ueki IF, Lausier JA, Nadel JA. IL-4 induces mucin gene expression and goblet cell metaplasia *in vitro* and *in vivo. J Immunol* 1999;162:6233–6237.
29. Chen Y, Thai P, Zhao YH, Ho YS, DeSouza MM, Wu R. Stimulation of airway mucin gene expression by interleukin (IL)-17 through IL-6 paracrine/autocrine loop. *J Biol Chem* 2003;278:17036–17043.
30. Reader JR, Hyde DM, Schelegle ES, Aldrich MC, Stoddard AM, McLane MP, Levitt RC, Tepper JS. Interleukin-9 induces mucous cell metaplasia independent of inflammation. *Am J Respir Cell Mol Biol* 2003;28:664–672.
31. Busse PJ, Zhang TF, Srivastava K, Lin BP, Schofield B, Sealfon SC, Li XM. Chronic exposure to TNF-alpha increases airway mucus gene expression *in vivo. J Allergy Clin Immunol* 2005;116:1256–1263.
32. Yanagihara K, Seki M, Cheng PW. Lipopolysaccharide induces mucus cell metaplasia in mouse lung. *Am J Respir Cell Mol Biol* 2001;24:66–73.
33. Chen Y, Zhao YH, Wu R. Differential regulation of airway mucin gene expression and mucin secretion by extracellular nucleotide triphosphates. *Am J Respir Cell Mol Biol* 2001;25:409–417.
34. Atherton HC, Jones G, Danahay H. IL-13–induced changes in goblet cell density of human bronchial epithelial cell cultures: MAP kinase and phosphatidylinositol 3-kinase regulation. *Am J Physiol Lung Cell Mol Physiol* 2003;285:L730–L739.
35. Allahverdian S, Harada N, Singhera GK, Knight DA, Dorscheid DR. Secretion of IL-13 by airway epithelial cells enhances epithelial repair via HB-EGF. *Am J Respir Cell Mol Biol* 2008;38:153–160.
36. Howell DCJ, Goldsack NR, Marshall RP, McAnulty RJ, Starke R, Purdy P, Laurent GJ, Chambers RC. Direct thrombin inhibition reduces lung collagen, accumulation, and connective tissue growth factor mRNA levels in bleomycin-induced pulmonary fibrosis. *Am J Pathol* 2001;159:1383–1395.
37. Roche N, Striling RG, Lim S, Oliver BG, Chung KF. Regulation of protease-activated receptor-1 in mononuclear cells by neutrophil proteases. *Respir Med* 2003;97:228–233.
38. Yufu T, Hirano K, Bi D, Hirano M, Nishimura J, Iwamoto Y, Kanaide H. Rac1 regulation of surface expression of protease-activated receptor-1 and responsiveness to thrombin in vascular smooth muscle cells. *Arterioscler Thromb Vasc Biol* 2005;25:1506–1511.
39. Paing MM, Johnston CS, Siderovski DP, Trejo J. Clathrin adaptor AP2 regulates thrombin receptor constitutive internalization and endothelial cell resensitization. *Mol Cell Biol* 2006;26:3231–3242.
40. Cavarra E, Bartalesi B, Lucattelli M, Fineschi S, Lunghi B, Gambelli F, Ortiz LA, Martorana PA, Lungarella G. Effects of cigarette smoke in mice with different levels of alpha(1)-proteinase inhibitor and sensitivity to oxidants. *Am J Respir Crit Care Med* 2001;164:886–980.
41. Bartalesi B, Cavarra E, Fineschi S, Lucattelli M, Lunghi B, Martorana PA, Lungarella G. Different lung responses to cigarette smoke in two strains of mice sensitive to oxidants. *Eur Respir J* 2005;25:15–22.
42. Renesto P, Si-Tahar M, Moniatte M, Balloy V, Van Dorsselaer A, Pidard D, Chignard M. Specific inhibition of thrombin-induced cell activation by the neutrophil proteinases elastase, cathepsin g, and proteinase 3: evidence for distinct cleavage sites within the amino-terminal domain of the thrombin receptor. *Blood* 1997;89:1944–1953.
43. Barnes PJ, Chung KF, Page CP. Inflammatory mediators of asthma: an update. *Pharmacol Rev* 1998;50:515–596.
44. Kohiri K, Ueki IF, Nadel JA. Neutrophil elastase induces mucin production by ligand-dependent epidermal growth factor receptor activation. *Am J Physiol Lung Cell Mol Physiol* 2002;283:L531–L540.
45. Uehara A, Muramoto K, Takada H, Sugawara S. Neutrophil elastase proteinases activate human nonepithelial cells to produce non inflammatory cytokines through protease-activated receptor-2. *J Immunol* 2003;170:5690–5696.
46. Wang H, Yi T, Zheng Y, He S. Induction of monocyte chemoattractant protein-1 release from A549 cells by agonists of protease-activated receptor-1 and -2. *Eur J Cell Biol* 2007;86:233–242.
47. Li T, He S. Induction of IL-6 release from human T cells by PAR-1 and PAR-2 agonists. *Immunol Cell Biol* 2006;84:461–466.